Title	Frequency modulation atomic force microscopy in ambient environments utilizing robust feedback tuning
Author(s)	Kilpatrick, J. I.; Gannepalli, A.; Cleveland, J. P.; Jarvis, Suzi
Publication date	2009-02-02
Publication information	Review of Scientific Instruments, 80 (2): 023701-023701-6
Publisher	American Institute of Physics
Item record/more information	http://hdl.handle.net/10197/4241
Publisher's statement	The following article appeared in Review of Scientific Instruments, 80 : 023701 (2009) and may be found at http://link.aip.org/link/doi/10.1063/1.3073964. The article may be downloaded for personal use only. Any other use requires prior permission of the author and the American Institute of Physics.
Publisher's version (DOI)	http://dx.doi.org/10.1063/1.3073964

AIP | Review of Scientific Instruments

Frequency modulation atomic force microscopy in ambient environments utilizing robust feedback tuning

J. I. Kilpatrick, A. Gannepalli, J. P. Cleveland, and S. P. Jarvis

Citation: Rev. Sci. Instrum. **80**, 023701 (2009); doi: 10.1063/1.3073964
View online: http://dx.doi.org/10.1063/1.3073964
View Table of Contents: http://rsi.aip.org/resource/1/RSINAK/v80/i2
Published by the American Institute of Physics.

Frequency modulation atomic force microscopy in ambient environments utilizing robust feedback tuning

J. I. Kilpatrick,[1] A. Gannepalli,[2] J. P. Cleveland,[2] and S. P. Jarvis[1]
[1]*Conway Institute, University College Dublin, Belfield, Dublin 4, Ireland*
[2]*Asylum Research, 6310 Hollister Ave., Santa Barbara, California 93117, USA*

(Received 22 August 2008; accepted 4 January 2009; published online 2 February 2009)

Frequency modulation atomic force microscopy (FM-AFM) is rapidly evolving as the technique of choice in the pursuit of high resolution imaging of biological samples in ambient environments. The enhanced stability afforded by this dynamic AFM mode combined with quantitative analysis enables the study of complex biological systems, at the nanoscale, in their native physiological environment. The operational bandwidth and accuracy of constant amplitude FM-AFM in low Q environments is heavily dependent on the cantilever dynamics and the performance of the demodulation and feedback loops employed to oscillate the cantilever at its resonant frequency with a constant amplitude. Often researchers use *ad hoc* feedback gains or instrument default values that can result in an inability to quantify experimental data. Poor choice of gains or exceeding the operational bandwidth can result in imaging artifacts and damage to the tip and/or sample. To alleviate this situation we present here a methodology to determine feedback gains for the amplitude and frequency loops that are specific to the cantilever and its environment, which can serve as a reasonable "first guess," thus making quantitative FM-AFM in low Q environments more accessible to the nonexpert. This technique is successfully demonstrated for the low Q systems of air ($Q \sim 40$) and water ($Q \sim 1$). In addition, we present FM-AFM images of MC3T3-E1 preosteoblast cells acquired using the gains calculated by this methodology demonstrating the effectiveness of this technique. © *2009 American Institute of Physics.* [DOI: 10.1063/1.3073964]

I. INTRODUCTION

Frequency modulation atomic force microscopy (FM-AFM) utilizes the detection of changes in the resonant frequency of an oscillating cantilever due to conservative force gradients arising from tip-sample interactions, which can be measured with extreme sensitivity. A frequency feedback loop is employed to ensure that the motion of the cantilever tip is phase shifted by 90° from the drive signal, i.e., the cantilever is oscillated at its resonant frequency irrespective of any tip-sample interaction.[1] When operated in constant amplitude mode (where the amplitude of the cantilever is maintained at a fixed value), through the addition of a second feedback loop, changes in energy dissipation arising from dissipative tip-sample interactions can also be observed by monitoring the excitation amplitude (proportional to the driving force). Provided that the cantilever is oscillated precisely at resonance and at constant amplitude, then the contributions from the conservative and dissipative interactions can be formally decoupled,[2–4] allowing insight into the nature of a measured interaction. The treatment of FM-AFM data relies on a static approximation, whereby the cantilever motion is assumed to be in an equilibrium state, free from transients, and that the frequency and amplitude feedback loops perform ideally.[5] It is therefore imperative to understand the cantilever dynamics and evaluate the performance of the demodulation and feedback loops in order to determine the effective bandwidth of FM-AFM for a given environment. This is of particular importance when operating in liquid environments where the motion of the cantilever is highly damped.

FM-AFM has traditionally been applied to the study of surfaces under ultrahigh vacuum (UHV), where atomic resolution is routinely obtained[6] and atomic scale chemical identification by force spectroscopy has been demonstrated.[7] Recently there has been increasing interest in the application of this technique to biological samples in liquid environments. The ability to probe large force gradients quantitatively, without mechanical instability, while maintaining high force sensitivity has enabled quantitative studies of the unfolding of proteins,[8] water structure at biological membrane interfaces,[9] and imaging of lipid ion networks.[10] Recent developments in AFM instrumentation have also enabled true atomic resolution imaging using FM-AFM while operating in liquid where the low Q results in a reduction in force sensitivity.[11]

The quantitative implementation of FM-AFM requires accurate determination of both the frequency and amplitude of the cantilever oscillations in response to tip-sample interactions. This requires good feedback loop performance (fast tracking and minimal error) and a mechanism for actuating the cantilever, which does not alter its dynamics. Piezoactivation, commonly used to actuate cantilevers in dynamic AFM, is generally unsuitable for FM-AFM in liquid environments since it often excites mechanical and acoustic resonances within the system in addition to that of the cantilever.[12] Whereas piezoactivation generally involves ex-

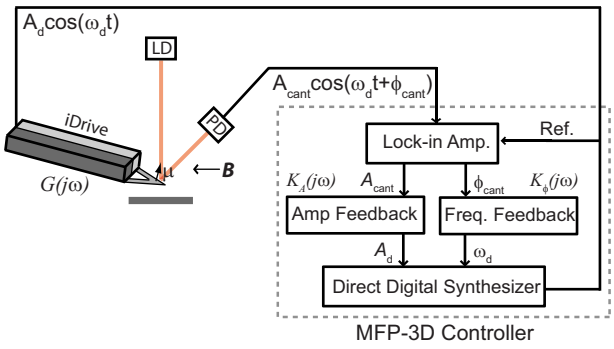

FIG. 1. (Color online) Schematic showing the experimental setup. Components within the dashed line are elements of the MFP-3D controller (Asylum Research, USA). The iDrive™ cantilever is electrically divided to allow current to flow through the v-shaped cantilever. The magnetic moment μ interacts with the static magnetic field B to provide the force to actuate the cantilever.

citation of the cantilever by motion of the attached chip, magnetic activation allows directed activation of the cantilever without an associated chip motion.[13,14] This generally results in cantilever dynamics free from the influence of actuation and proves suitable for quantitative FM-AFM.

The influence of feedback tuning upon the imaging performance of FM-AFM has been the subject of a number of studies.[15,16] Such investigations primarily deal with the impact of a given set of feedback parameters upon performance rather than addressing the issue of how to derive appropriate gains for a given cantilever environment in a robust manner. Gildemeister *et al.*[17] described the tuning of a phase locked loop to track changes in tuning fork frequency for a low temperature UHV system, where the bandwidth of the feedback loop is set to match that of the cantilever. While this approach is suitable for high Q systems ($Q > 100\,000$) where the cantilever bandwidth is low, it is often unsuitable for low Q systems (ambient environments) as the bandwidth of the cantilever often exceeds the stable bandwidth of the feedback loop.

When implementing the feedback loops in an FM-AFM experiment, researchers often use *ad hoc* feedback gains or instrument default values resulting in gains that are often not directly associated with the cantilever dynamics for a given environment. The failure to use appropriate control parameters for the frequency and amplitude loops can result in an inability to quantify experimental data, imaging artifacts, and damage to the tip and/or sample. To alleviate this situation we present here a methodology to determine stable feedback gains for the frequency and amplitude loops that are specific to the given cantilever environment, which can serve as a reasonable "first guess" for subsequent fine tuning.

II. MATERIALS AND METHODS

Figure 1 shows a schematic of the experimental setup. In this example we use iDrive™ combined with a MFP-3D SA system (Asylum Research, USA) to actuate an AR-iDrive-N02 (Asylum Research, USA) cantilever with a typical spring constant of ~ 0.6 N m^{-1}. All cantilever response experiments are carried out in air and Milli-Q water at a separation of 2 μm from a freshly cleaved muscovite mica surface (Agar Scientific, U.K.). For this system, cantilever actuation is achieved by passing an electric current, i, through a triangular cantilever forming a current loop with a magnetic moment, μ, perpendicular to the plane of the cantilever. When placed in a static magnetic field, B, at some angle to μ, a force, F, proportional to i is generated, tending to align B and μ.[18] This method of actuation results in a fundamental mode cantilever response that is free from spurious phase and amplitude influences and so is suitable for quantitative FM-AFM.[18,19]

Frequency and amplitude demodulation is realized using a quadrature digital lock-in amplifier utilizing the cantilever excitation signal as a reference. The cantilever amplitude A_{cant} and phase ϕ_{cant} signals from the lock-in amplifier are sampled at 100 kHz and used as the inputs to digital amplitude and frequency proportional-integral (PI) feedback loops, respectively. The feedback outputs, namely, the drive amplitude and frequency, are input into a direct digital synthesizer, which generates the sinusoidal signal used to oscillate the cantilever. All digital components are contained within the MFP-3D controller (Asylum Research, USA) and are controlled by a custom software written in IGOR PRO (Wavemetrics, USA).

Cell imaging experiments were conducted in magnetic activation dynamic (MAD) mode[13] using PPP-FM cantilevers (Nanosensors, Switzerland) with a typical spring constant of ~ 1.1 N m^{-1}. A magnetic particle (MQP-14–12, Magnequench, Germany) was attached to the backside of the cantilever using an epoxy (EPO-TEK 353ND, Promatek, U.K.) with the aid of a light microscope and micromanipulation. Actuation was achieved by modulated magnetic field provided by a coil positioned beneath the sample.

Prior to cell imaging, MC3T3-E1 preosteoblast cells (ATCC, U.K.) were cultured on a glass slide in Minimum Essential Medium Eagle Alpha Modification (Sigma-Aldrich, U.K.). Live cell samples were cultured for a period of 2 days, washed in phosphate buffered saline (PBS) (two times) (Sigma-Aldrich, U.K.), and then imaged in PBS at room temperature. Fixed cell samples were cultured for a period of 2 days and then prepared by washing (two times) in PBS and fixing with 4% *para*-formaldehyde (Sigma-Aldrich, U.K.) for at least 30 min at room temperature. Samples were then washed in PBS (three times) and stored at 4 °C overnight. Fixed cell samples were then imaged in PBS at room temperature.

III. FEEDBACK PARAMETER DETERMINATION

The determination of suitable feedback parameters for the frequency and amplitude loops in FM-AFM is highly dependent on the cantilever dynamics, which is in turn intricately related to its mechanical properties in a given environment. Here we present a methodology to determine the gain parameters that will result in stable operation of the feedback loops with a reasonable performance for a given environment. It is important to note that these gains are not optimal but just a good first guess, which can be further tuned as required. The calculation of gain parameters requires knowledge of the mechanical properties of the cantilever, which

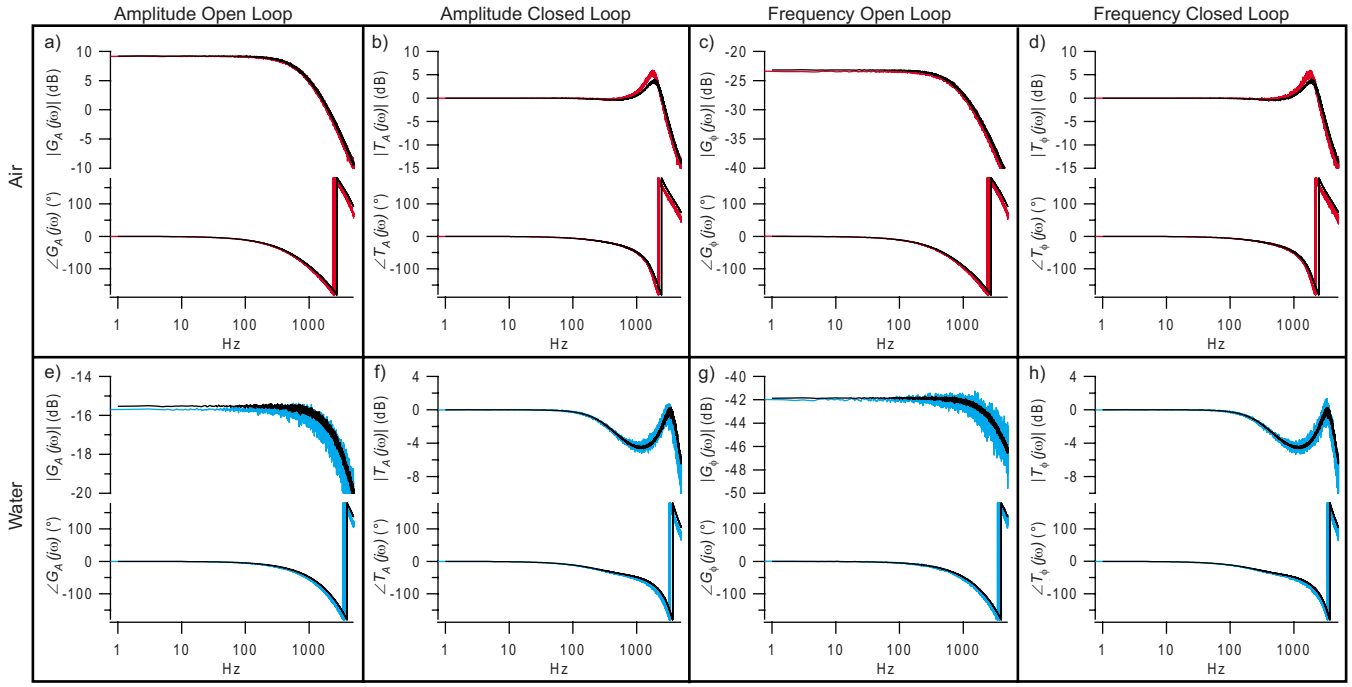

FIG. 2. (Color online) Open and closed loop transfer functions for the amplitude and frequency feedback loops at a separation of 2 μm from a freshly cleaved mica surface. Black—model data; red—air response (ω_0=65.998 kHz, Q=40.0, and A_{cant}=12 nm); and blue—water response (ω_0=21.002 kHz, Q=1.5, and A_{cant}=10 nm). Data represent the average of 30 samples. Bode plots are shown for (a) open loop amplitude response air, (b) closed loop amplitude response air (gains $[P,I]$=0.621, 2028.6), (c) open loop frequency response air, (d) closed loop frequency response air (gains $[P,I]$=25.824, 84 372.7), (e) open loop amplitude response water, (f) closed loop amplitude response water (gains $[P,I]$=3.880, 18 246.5), (g) open loop frequency response water, and (h) closed loop frequency response water (gains $[P,I]$=78.919, 371 128.0).

are obtained during the course of routine experimental setup for dynamic AFM. The frequency response of the lock-in amplifier, which can be determined offline, must also be taken into account and is deemed a constant specific to the instrumentation.

In order to determine the mechanical properties of the cantilever, a Brownian fluctuation spectrum is obtained and fitted with a damped harmonic oscillator model yielding the cantilever's natural resonant frequency ω_0 for a given environment. A frequency sweep centered about ω_0 with a constant drive amplitude A_d is then performed and $A_{\text{cant}}(\omega)$ and $\phi_{\text{cant}}(\omega)$ are recorded. It is instructive to note that $\phi_{\text{cant}}(\omega_0)=\pi/2$ is the setpoint of the frequency feedback loop controlling the drive frequency ω_d, thereby tracking any changes in $\omega_0(\approx\omega_d)$ due to conservative tip-sample interactions. The amplitude feedback loop strives to keep A_{cant} constant at a given setpoint by changing A_d in response to dissipative tip-sample interactions. The system can then be modeled as

$$\mathbf{G}_A(j\omega)=\frac{A_{\text{cant}}(\omega)}{A_d(\omega)}=\left[\frac{A_{\text{cant}}(\omega_0)}{A_d(\omega_0)}\right]\frac{1}{j\omega+B}\mathbf{G}_{\text{lock-in}}(\omega), \quad (1a)$$

$$\mathbf{G}_\phi(j\omega)=\frac{\phi_{\text{cant}}(\omega)}{\omega_d(\omega)}=\left(\left.\frac{\partial\phi_{\text{cant}}}{\partial\omega_d}\right|_{\omega_d=\omega_0}\right)\frac{1}{j\omega+B}\mathbf{G}_{\text{lock-in}}(\omega), \quad (1b)$$

where all the required information can be obtained from the frequency sweep data and $\boldsymbol{G}_{\text{lock-in}}(\omega)$ represents the frequency response of the lock-in amplifier. It should be noted that ω_0 is not located at the peak amplitude response for low Q systems.[20] Here B is the bandwidth of amplitude and phase dynamics for the cantilever and is approximated[1] as $B=\omega_0/2Q$ where

$$Q=\left(\frac{\omega_0}{2}\right)\left(\left.\frac{\partial\phi_{\text{cant}}}{\partial\omega_d}\right|_{\omega_d=\omega_0}\right). \quad (2)$$

For a PI feedback loop of the form $\boldsymbol{K}(j\omega)=K_P+K_I/j\omega$, we employ the Ziegler–Nichols[21] tuning method to determine the first guess values for the proportional K_P and integral K_I gains. The gain margin K_{pu} for the feedback loop stability and the oscillation period τ_{pu} at the stability limit can be estimated from the open loop transfer function models [Eqs. (1a) and (1b)] as $K_{\text{pu}}=(|\boldsymbol{G}(j\omega_{180})|)^{-1}$ and $\tau_{\text{pu}}=2\pi/\omega_{180}$ such that $\angle\boldsymbol{G}(j\omega_{180})=-180°$, where $|\,|$ and $\angle$ represent the magnitude and phase of the transfer function, respectively. The feedback loop gain parameters according to the Ziegler–Nichols[21] heuristic are given by $K_P=K_{\text{pu}}/2.2$ and $K_I=1.2\times K_P/\tau_{\text{pu}}$. Once the feedback gains have been determined, the closed loop response of the feedback loops can be modeled as

$$\mathbf{T}(j\omega)=\frac{\mathbf{G}(j\omega)\mathbf{K}(j\omega)}{1+\mathbf{G}(j\omega)\mathbf{K}(j\omega)}. \quad (3)$$

In the results presented in Fig. 2 the transfer functions are measured by applying a chirp function to the relevant control parameter and the detected response is evaluated by the calculation of a cross correlation function. Analysis of the closed loop response is performed with both amplitude and frequency loops active, while one setpoint is modulated the other remains constant. This methodology allows a more relevant response of the cantilever to perturbations to be ob-

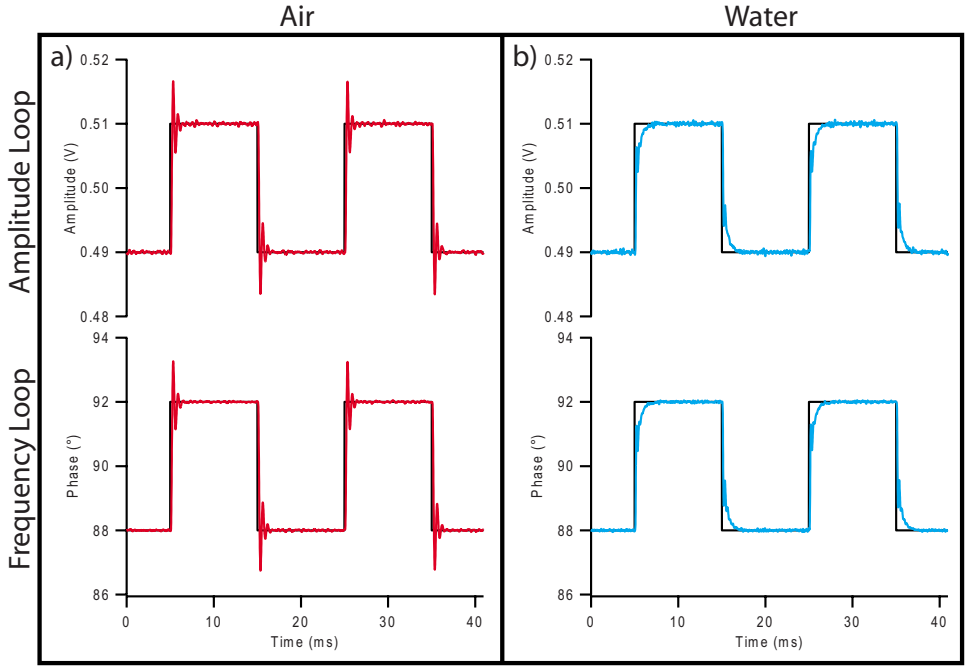

FIG. 3. (Color online) Closed loop step response of the cantilever amplitude loop (red) and frequency loop (blue) to setpoint modulation (black) in (a) air (ω_0=65.998 kHz, Q=40.0, and A_{cant}=12 nm) and (b) water (ω_0=20.978 kHz, Q=1.5, A_{cant}=8 nm) at a separation of 2 μm from a freshly cleaved mica surface. Data represent the average of 500 samples. Air amplitude loop gains $[P,I]$=0.621, 2028.6. Air frequency loop gains $[P,I]$=25.824, 84 372.7. Water amplitude loop gains $[P,I]$=3.946, 18 624.3. Water frequency loop gains $[P,I]$=81.762, 385 948.0. Maximum overshoot for amplitude and frequency loops in air is $<2\%$. Maximum overshoot for amplitude and frequency loops in water is $<0.2\%$. Air: amplitude loop IAE=3.5×10^{-4}, frequency loop IAE=3.1×10^{-4}, and settling time=1.3 ms (86 cantilever oscillations). Water: amplitude loop IAE=3.8×10^{-4}, frequency loop IAE=3.6×10^{-4}, and settling time =1.5 ms (31 cantilever oscillations). All IAE values are normalized by the setpoint step magnitude.

tained since both loops are required to be active during constant amplitude FM-AFM experiments.

IV. EXPERIMENTAL RESULTS

Figure 2 shows the open loop $\boldsymbol{G}(j\omega)$ and closed loop $\boldsymbol{T}(j\omega)$ responses of a cantilever in air and Milli-Q water for the frequency and amplitude loops. It is evident that the models described in Eqs. (1a) and (1b) are in good agreement with the measured responses. The PI gains calculated by the Ziegler–Nichols[21] method result in reasonable closed loop performance and while these parameters may not represent optimal control, they do consistently yield a stable state that can be further tuned if required. It can be seen that the nominal PI gains in air and water differ by an order of magnitude and such variance in the gains illustrates the need for careful consideration of the cantilever dynamics and instrumental influences in determining the required parameters for FM-AFM operation in low Q environments. The accurate modeling of the system in these low Q environments also allows the direct determination of an upper limit in the operational bandwidth of FM-AFM.

In order to assess the closed loop feedback performance in the time domain, a setpoint step response was measured for each of the loops. Here the setpoint of the feedback loop is instantaneously varied by a small amount and the error signal is monitored as a function of time. Figure 3 shows the closed loop time response of A_{cant} and ϕ_{cant} in response to a modulation of the amplitude and frequency feedback setpoints. In each case one setpoint is modulated while the other remains constant. The time domain response of the feedback loops in air [Fig. 3(a)] shows a maximum overshoot of $<2\%$ with a settling time of 1.3 ms (86 cantilever cycles). The normalized integral absolute errors (IAEs) for these transitions were 3.5×10^{-4} and 3.1×10^{-4} for the amplitude and frequency loops, respectively. Values are normalized by the magnitude of the setpoint modulation. The closed loop time domain response in water [Fig. 3(b)] demonstrates $<0.2\%$ maximum overshoot and a settling time of 1.5 ms (31 cantilever oscillations). The normalized IAEs for the amplitude and frequency loop step response were 3.8×10^{-4} and 3.6×10^{-4}, respectively. The dead time for the feedback system was 80 μs (eight DSP cycles).

It is evident that the cantilever environment dominates the system response for low Q behavior with implications for both the effective bandwidth and force sensitivity. The feedback parameters determined by the robust tuning algorithm presented here demonstrate excellent steady state error performance and while the time response of the system is of the order of multiple cantilever cycles, this is attributed to the low bandwidth achievable in these low Q systems. Consequently, the effective bandwidth of FM-AFM experiments under such conditions must be reduced accordingly in order to maintain a quantitative response. The DSP implementation of FM-AFM presented here has the added advantage of allowing access to error signals for each of the feedback loops in real time, allowing the user to continuously monitor the effectiveness of the feedback loops for a given scanning speed. Benefits also arise from the use of a quadrature digital lock-in amplifier allowing direct access to in-phase (i_{cant}) and quadrature (q_{cant}) signals generated during detection. For low

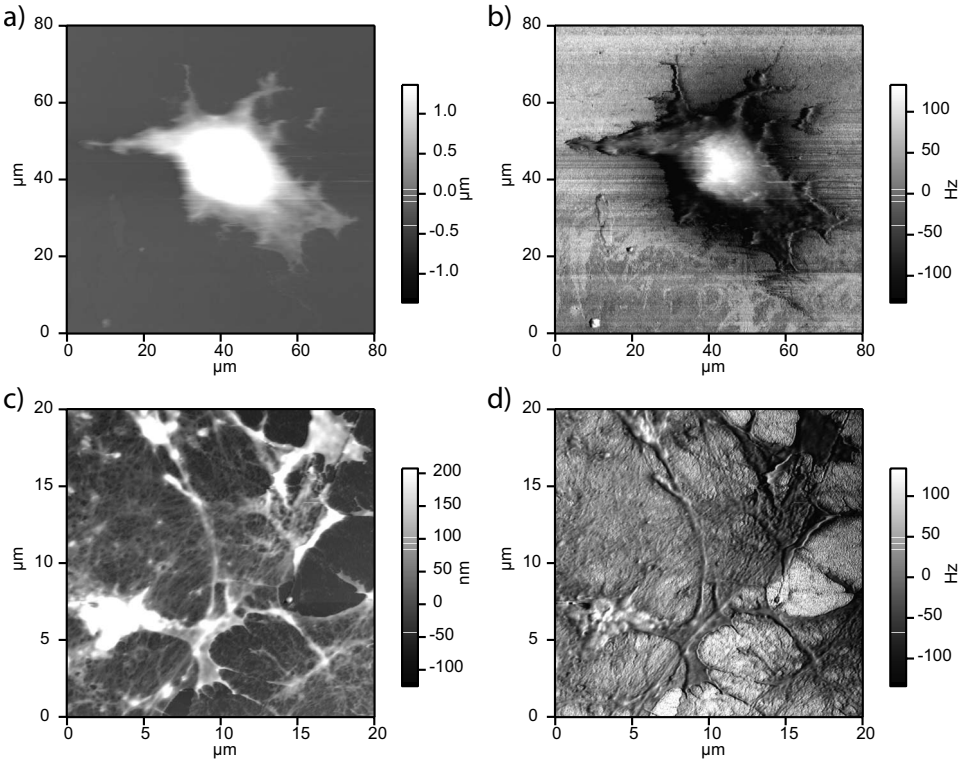

FIG. 4. FM-AFM images of MC3T3-E1 preosteoblast cells on a glass substrate in PBS buffer solution. Images were acquired using calculated gains for the amplitude and frequency loops without modification. Dissipation was used as the input to the tip-sample distance control loop. An 80 μm image of a live cell sample, height (a) and frequency shift (b), acquired using PPP-FM cantilever in MAD mode (ω_0=16.927 kHz, Q=4.8, A_{cant}=92 nm, and tip velocity =100 μm s^{-1}). Amplitude loop gains $[P,I]$=2.596, 10 337.0, frequency loop gains $[P,I]$=37.465, 149 170. Amplitude loop response [setpoint, average, σ]=0.8, 0.800, and 0.003 V. Phase loop response [setpoint, average, σ]=90°, 90.0°, and 0.3°. A 20 μm image of a fixed cell sample, height (c) and frequency shift (d), acquired using PPP-FM cantilever in MAD mode (ω_0=12.350 kHz, Q=4.2, A_{cant}=88 nm, and tip velocity=25 μm s^{-1}). Amplitude loop gains $[P,I]$=0.637, 914.29, frequency loop gains [P,I]=16.787, 24 080. Amplitude loop response [setpoint, average, σ] =0.8, 0.800, 0.007 V. Phase loop response (setpoint, average, σ) =90°, 90.0°, and 1.3°.

Q systems, where the phase noise is relatively large,[1] the potential to use i_{cant} as the error signal represents an advantage over the use of ϕ_{cant} since i_{cant} and q_{cant} each contain equal noise contributions from the thermal motion of the cantilever and $\phi_{\text{cant}}=\tan^{-1}(q_{\text{cant}}/i_{\text{cant}})$.

Recently it has been reported that the addition of Q control, where an additional feedback loop is employed to artificially increase the Q of the cantilever, to a constant excitation FM-AFM system resulted in enhanced sensitivity and a reduction in the tip-sample forces when operating in liquid.[22,23] From the above analysis it is evident that an increase in Q of the system without a corresponding change in the resonant frequency of the cantilever would lead to a reduction in the bandwidth of the cantilever and, as such, may further limit the effective bandwidth of a given system. Alternatively, increasing both the Q and the resonant frequency of the system by using stiffer cantilevers may lead to an increase in the effective bandwidth while maintaining the benefit of enhancement in force sensitivity. The use of such cantilevers offers the additional benefit of being able to probe large force gradients without mechanical instability. In this case the limiting element in determining the effective bandwidth when using very stiff ($k\sim 20$ N m^{-1}, $\omega_0 \sim 125$ kHz, $Q\sim 6.5$) cantilevers in liquid environments is likely to be commercial scanners, which typically have resonant frequencies below 5 kHz.

In order to demonstrate the effectiveness of the proposed technique for low Q biomaterials applications, both living and fixed cell samples were imaged in solution using constant amplitude FM-AFM in MAD mode. Figure 4 shows height and frequency shift images of live [Figs. 4(a) and 4(b)] and fixed [Figs. 4(c) and 4(d)] MC3T3-E1 preosteoblast cells on a glass substrate in PBS buffer solution. Dissipation was used as the input to the tip-sample distance control loop. Feedback gains calculated for the amplitude and frequency loops were used without any modification. For the live cell, the amplitude response showed a standard deviation σ of 0.4% and the phase response showed σ=0.3°. For the fixed cell, the amplitude response showed σ=0.9% and the phase response showed σ=1.3°. All values were determined for the entire image (512×512 pixels). Errors in the amplitude and frequency loops were minimal, demonstrating effective choice of appropriate gains by the algorithm.

V. CONCLUSION

The application of a robust parameter identification routine for constant amplitude FM-AFM in low Q environments has been successfully demonstrated for operation in air ($Q \sim 40$) and in water ($Q\sim 1$). By modeling the mechanical response of the cantilever and the instrumental characteristics, the parameters required for stable feedback loop tuning are able to be routinely calculated for low Q systems showing reasonable performance. These parameters represent a

good "first guess" and allow for further tuning to reach optimal feedback control conditions. The measured open and closed loop responses of the FM-AFM feedback system have been shown to match model calculations in air and water. These models also allow the calculation of the operational bandwidth, which is an important (and often ignored) parameter to consider in experimental design since exceeding this can result in an inability to quantify experimental data imaging artifacts and tip and/or sample damage. Time domain analysis was also performed in order to assess the performance of the feedback loops. Stable performance was always observed with good tracking for low Q systems. Application to the study of biomaterials was demonstrated by imaging both live and fixed cells in a liquid environment using gains calculated by the algorithm presented herein. Assessment of the amplitude and phase errors in these images showed that the frequency and amplitude loops were able to track the cantilever response with minimal error while imaging under physiologically relevant conditions. While the application of the Ziegler–Nichols[21] tuning method in this study may not represent the optimal choice of parameters for a given low Q system, it does consistently yield stable feedback conditions with reasonable performance. Future work may include the implementation of more advanced and/or adaptive feedback tuning methods in order to obtain values that are closer to optimum.

ACKNOWLEDGMENTS

This research was supported by the Science Foundation Ireland Research Grant No. 07/IN1/B931 and collaboration between University College Dublin and Asylum Research. The authors would also like to thank Akitoshi Toda (Olympus) for supplying iDrive levers with high spring constants and Geraldine Kelly (University College Dublin) for preparation of the cell samples.

[1] T. R. Albrecht, P. Grutter, D. Horn, and D. Rugar, J. Appl. Phys. **69**, 668 (1991).
[2] B. Gotsmann, C. Seidel, B. Anczykowski, and H. Fuchs, Phys. Rev. B **60**, 11051 (1999).
[3] H. Hölscher, B. Gotsmann, W. Allers, U. D. Schwarz, H. Fuchs, and R. Wiesendanger, Phys. Rev. B **64**, 075402 (2001).
[4] J. E. Sader, T. Uchihashi, M. J. Higgins, A. Farrell, Y. Nakayama, and S. P. Jarvis, Nanotechnology **16**, S94 (2005).
[5] J. Kokavecz, Z. Tóth, Z. L. Horváth, P. Heszler, and Á. Mechler, Nanotechnology **17**, S173 (2006).
[6] F. J. Giessibl, Rev. Mod. Phys. **75**, 949 (2003).
[7] Y. Sugimoto, P. Pou, M. Abe, P. Jelinek, R. Perez, S. Morita, and O. Custance, Nature (London) **446**, 64 (2007).
[8] M. J. Higgins, J. E. Sader, and S. P. Jarvis, Biophys. J. **90**, 640 (2006).
[9] T. Fukuma, M. J. Higgins, and S. P. Jarvis, Biophys. J. **92**, 3603 (2007).
[10] T. Fukuma, M. J. Higgins, and S. P. Jarvis, Phys. Rev. Lett. **98**, 106101 (2007).
[11] T. Fukuma, K. Kobayashi, K. Matsushige, and H. Yamada, Appl. Phys. Lett. **87**, 034101 (2005).
[12] X. Xu and A. Raman, J. Appl. Phys. **102**, 034303 (2007).
[13] S. P. Jarvis, A. Oral, T. P. Weihs, and J. B. Pethica, Rev. Sci. Instrum. **64**, 3515 (1993).
[14] S. M. Lindsay, Y. L. Lyubchenko, N. J. Tao, Y. Q. Li, P. I. Oden, J. A. DeRose, and J. Pan, J. Vac. Sci. Technol. A **11**, 808 (1993).
[15] J. Polesel-Maris and S. Gauthier, J. Phys.: Conf. Ser. **61**, 949 (2007).
[16] B. I. Kim, Rev. Sci. Instrum. **75**, 5035 (2004).
[17] A. E. Gildemeister, T. Ihn, C. Barengo, P. Studerus, and K. Ensslin, Rev. Sci. Instrum. **78**, 013704 (2007).
[18] A. Buguin, O. Du Roure, and P. Silberzan, Appl. Phys. Lett. **78**, 2982 (2001).
[19] S. P. Jarvis, Appl. Phys. A: Mater. Sci. Process. **72**, S129 (2001).
[20] J. E. Sader and S. P. Jarvis, Phys. Rev. B **74**, 195424 (2006).
[21] J. G. Ziegler and N. B. Nichols, J. Dyn. Control Syst. **115**, 220 (1993).
[22] D. Ebeling and H. Hölscher, J. Appl. Phys. **102**, 114310 (2007).
[23] D. Ebeling, H. Hölscher, and B. Anczykowski, Appl. Phys. Lett. **89**, 203511 (2006).